

# Energetic Proton Maps for the South Atlantic Anomaly

Gregory P. Ginet, Dan Madden, Bronislaw K. Dichter and Donald H. Brautigam

**Abstract**— A new set of flux intensity maps for energetic protons in the South Atlantic Anomaly (SAA) region is presented for the epoch 2000-2006 based on data from the Compact Environment Anomaly Sensor (CEASE) flown onboard the Tri-Service Experiment-5 (TSX-5) satellite in a 410 km x 1710 km, 69 degree inclination orbit. Maps for > 23 MeV, > 38 MeV, > 66 MeV and > 94 MeV protons have been constructed and boundary contours for 1/2 maximum, 1/10 maximum and 3 times the background standard deviation derived. Estimates are given of the integral energy spectra as a function of altitude from 400 km to 1650 km, an interval spanning the range where the controlling factor in the dynamics changes from the neutral density to the global magnetic field. The position of the maximum flux point is compared to that determined from earlier measurements in the 1994-1996 epoch and found to be consistent with the well-known westward drift.

## I. INTRODUCTION

DESPITE efforts to design space systems to survive the space radiation environment, modern spacecraft can still experience high rates of anomalies due to single event effects (SEEs) arising from cosmic rays and high-energy radiation belt protons. SEEs may range from nuisance effects requiring operator intervention to debilitating effects which lead to functional or total spacecraft loss. For satellites in low-Earth orbit (LEO) the dominant source of proton fluence in the absence of high-latitude solar proton events is the South Atlantic Anomaly (SAA). The SAA is the localized region at a fixed altitude where particles in the inner radiation belt reach their highest intensities as a result of the asymmetry of the Earth's magnetic field, which is closely approximated by a tilted, offset dipole in the inner magnetosphere. In many cases SEEs create high background counts which render sensors unusable during passage through the SAA. Operators who control affected space vehicles need to know how best to minimize the risk of anomalies which in

many cases simply means knowing, with a high degree of accuracy, when and where to turn systems on and off. The location of the SAA has often been determined by using proton intensity maps derived from the NASA AP radiation belt climatology models [1]. However, it is well known both from data and geomagnetic theory that as a result of the variations in the Earth's internal magnetic field the location of the energetic proton belts has changed significantly since the first models were made in the 1970's. The predominantly westward drift of the SAA is approximately 0.3 degrees/year [2], [3] – a magnitude which can lead to significant inaccuracies in the prediction of high-dose regions in LEO if old models are not updated. An improved set of single event effect maps (SEEMAPS) were constructed in 1998 from data taken by the Air Force's APEX and CRRES satellites during the epoch 1990-1996 [4].

In this paper we report on a new set of LEO proton flux intensity maps, contour levels and worst case spectra for the epoch 2000-2006 based on data from the Compact Environment Anomaly Sensor (CEASE) onboard the Tri-Service Experiment-5 (TSX-5) satellite. Besides being more up-to-date, the new maps expand the spectral coverage beyond the single energy offered ( $\sim > 50$  MeV) by the APEX/CRRES SEEMAPS.

## II. METHOD OF ANALYSIS

The TSX-5 spacecraft was launched on June 7, 2000 into a 410 x 1710 km, 69 degree inclination orbit and the CEASE instrument collected data for the entire mission until termination on July 5, 2006. The specifications and response of CEASE are described in detail elsewhere [5] – [7] and only a brief description of the particle sensors will be given here. CEASE is comprised of two dosimeters and a particle telescope, where the telescope consists of two coaxial Si solid-state detectors that measure the energy deposited in them by incident particles. Only telescope data were used to compute the maps presented here. The response of the telescope to incident protons was extensively modeled using the Monte-Carlo MCNPX computer code which simulates the passage of particles through material. The response was determined for protons with energies between 20 and 200 MeV and for angles of incidence up to 90 degrees from the center axis corresponding to the detector look direction. It was found that detection efficiency drops substantially starting in the range of 30 – 40 degrees depending on detector channel. Proton beam calibrations for the telescope, validating the computer model of the telescope response,

---

Manuscript received 20 July, 2007.

G. P. Ginet is with the Space Vehicles Directorate, Air Force Research Laboratory, Hanscom AFB, MA 01731 USA (email: [gregory.ginet@hanscom.af.mil](mailto:gregory.ginet@hanscom.af.mil)).

D. Madden is with the Institute for Scientific Research, Boston College, Boston, MA 02467 USA (email: [dan.madden@hanscom.af.mil](mailto:dan.madden@hanscom.af.mil)).

B. K. Dichter was with the Space Vehicles Directorate, Air Force Research Laboratory, Hanscom AFB, MA 01731 USA. He is now with Assurance Technology Corporation, Carlisle, MA 01741 (email: [dichter@assurtech.com](mailto:dichter@assurtech.com)).

D. H. Brautigam is with the Space Vehicles Directorate, Air Force Research Laboratory, Hanscom AFB, MA 01731 USA (email: [donald.brautigam@hanscom.af.mil](mailto:donald.brautigam@hanscom.af.mil)).

have not yet been performed. However, comparisons of the Monte Carlo derived results for the angular response of the telescope have been compared to results of a simple analytical model of a two element telescope. The agreement between the two different calculations is very good. Similarly, some simple Monte Carlo results on the energy response of the telescope have been checked against empirical calculations using range-energy tables and the known geometry of the telescope shielding material.

The pattern of energy loss by protons in the telescope detectors allowed us to compute geometric factors for four proton channels, corresponding to threshold energies of 23 MeV, 38 MeV, 66 MeV and 94 MeV. Uncertainties in the geometric factors and threshold energies due to the sensor modeling process were estimated by using different characterizations of the proton spectrum when integrating the channel response functions [7]. Maximum variations in the geometric factors (energy thresholds) were found to be of order 80% (50%), 24% (19%), 15% (8%) and 16% (13%) for the > 23, > 38, > 66 and > 94 MeV channels, respectively. Our simple application of the Monte-Carlo results assumes an incident isotropic flux which is not necessarily consistent with observations indicating distributions peaked about the direction of locally mirroring particles [8]. This direction is not always within the effective CEASE field of view. More will be said about the consequences of the CEASE look-direction in Section IV.

For each of the four proton channels the count rate data collected during the entire mission were corrected for dead-time effects and then sorted into a geographic grid of bin size 3 degrees longitude by 3 degrees latitude by 50 km altitude over the range 400 to 1650 km. All solar proton events (SPEs) were excluded to ensure the SAA maps were not contaminated by the transient proton population. A SPE was defined as the time interval when the NOAA GOES Space Environment Monitor (SEM) detector's > 10 MeV proton channel on the geosynchronous satellite measured greater than 10 protons/(cm<sup>2</sup> sec str). After SPE removal there were typically greater than 100 measurements per bin. A background count rate for each energy channel and altitude was determined by performing a Poisson fit to the distribution of count rates at intermediate latitudes outside of the anomaly but below latitudes where the telescope responds to high energy electrons in the horns of the outer belt. The background was subsequently subtracted from the channel data.

### III. RESULTS

#### A. Flux Intensity Maps

Maps of integral energy flux above the threshold energies of the four channels have been produced by first computing maps of the corrected count rates then dividing by the geometric factors estimated from the Monte Carlo modeling described above. Figure 1(a-d) displays maps for the > 38 MeV channel at four altitudes (400, 800, 1100, and 1650 km). Apparent in Fig. 1 (and all other channels) is a background level of count rates at the extreme northern and southern latitudes as a result of the telescope response to the high energy electrons populating the outer zone radiation belt and auroral regions. This effect is greatest in the > 66 MeV and > 94 MeV proton channels which are sensitive to electron energies of 0.83 MeV and 0.68 MeV, respectively, albeit with geometric factors four orders of magnitude less than those characterizing the proton response. Given the disparity in geometric factors it is reasonable to assume that the response in the anomaly is predominantly from protons.

Locations of maximum intensity are determined from both unsmoothed and smoothed data for each altitude and each channel. The smoothing is accomplished with a boxcar smoothing function applied to 3 consecutive bins. The square (cross) at the center of the SAA in Fig. 1 marks the location of the maximum for the smoothed (unsmoothed) data. Boundaries corresponding to the contour of 1/2 maximum (solid curve), 1/10 maximum (dotted curve) and 3 standard deviations above the background (dashed curve) are computed and translated into smooth functions of latitude and longitude.

Figure 2 (a-d) compares the contours of all the channels, > 23 MeV (solid curve), > 38 MeV (short dash curve), > 66 MeV (dot curve) and > 94 MeV (long dash curve) at four different altitudes (400, 800, 1100, and 1650 km). The extent of the anomaly grows substantially with altitude, and the boundaries for the higher energies are typically displaced to the northwest with respect to the lower energies. This feature is consistent with general observations of protons in the radiation belt, i.e. the distribution functions of higher energy particles tend to peak at lower magnetic shells than do those for lower energies [9]. Comparing the > 23 MeV with the > 94 MeV channel, the displacement can often be 5 degrees or greater indicating that "turn off" regions for sensitive satellite components could be significantly different depending on the proton energy level responsible for the anomalous behavior.

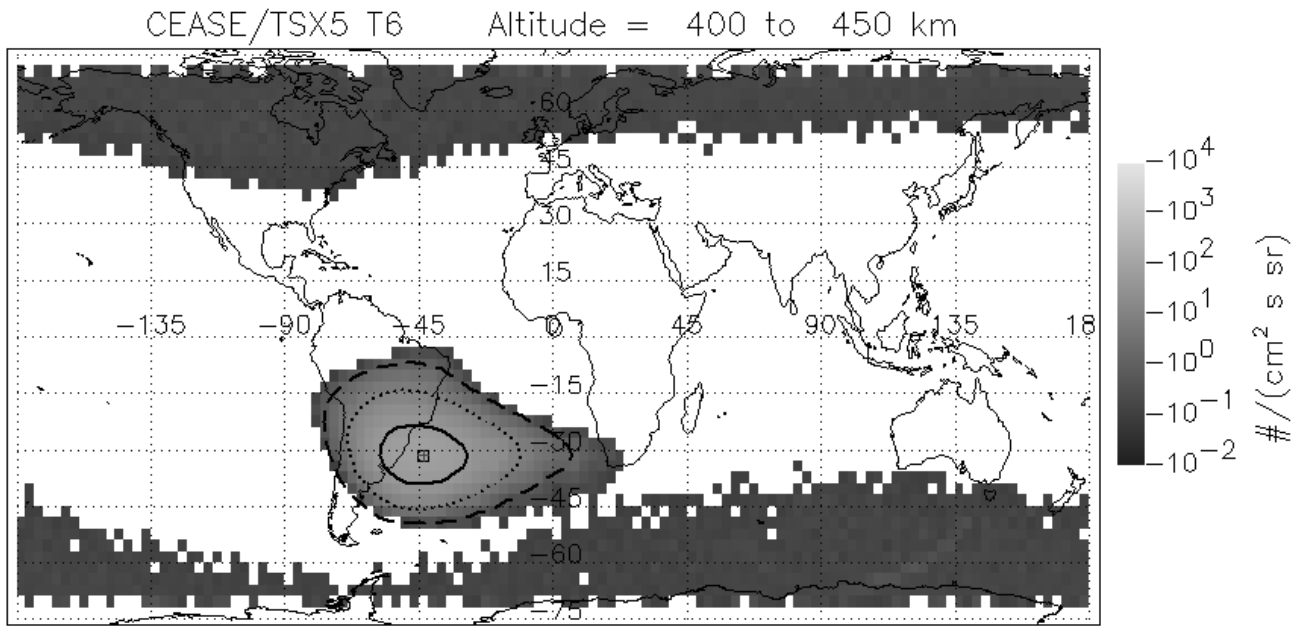


Fig. 1a. Flux intensity map for the > 38 MeV channel at 400 km altitude.

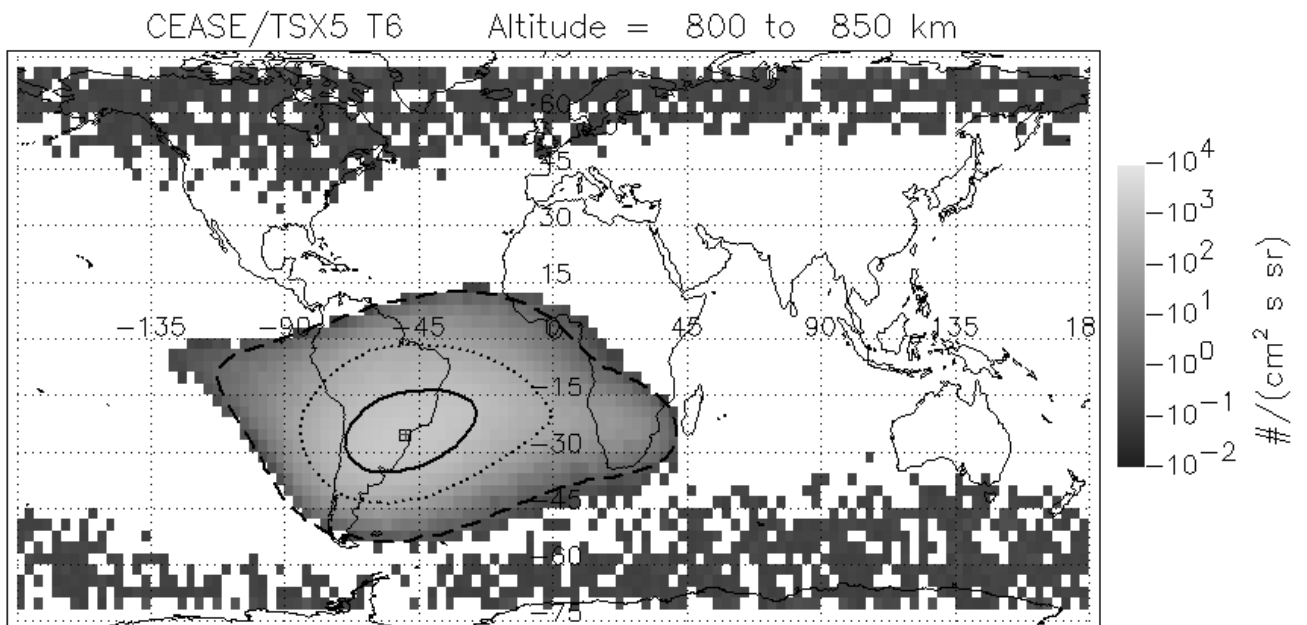


Fig. 1b. Flux intensity map for the > 38 MeV channel at 800 km altitude.

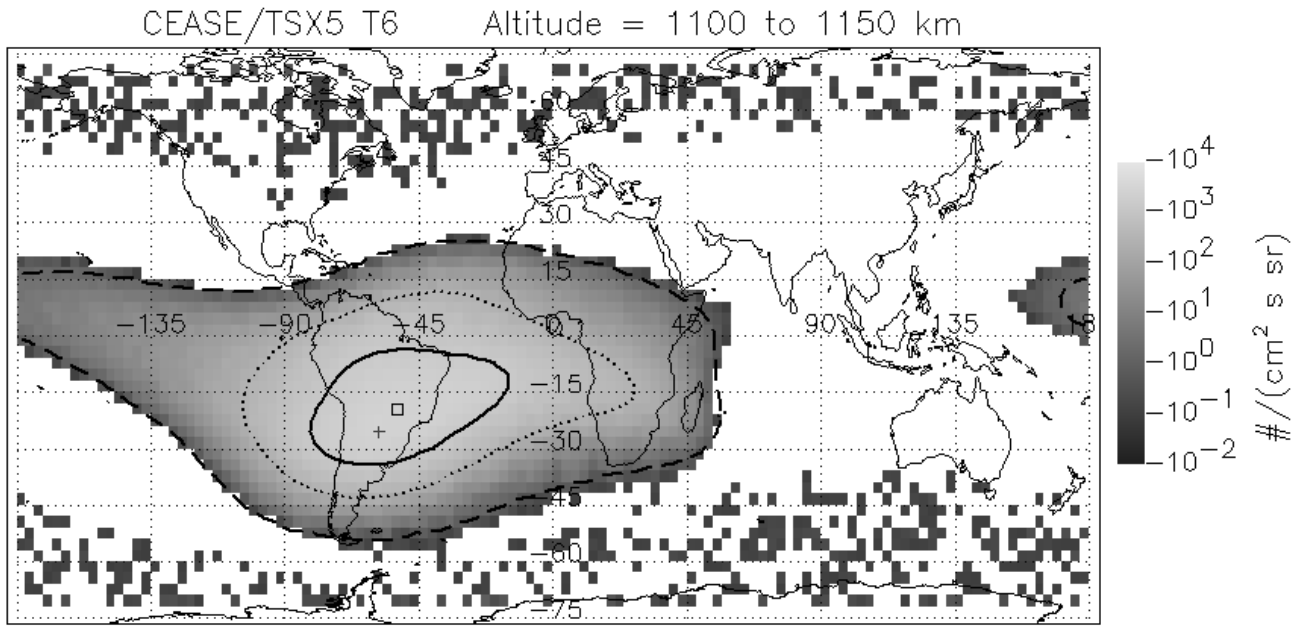


Fig. 1c. Flux intensity map for the > 38 MeV channel at 1100 km altitude.

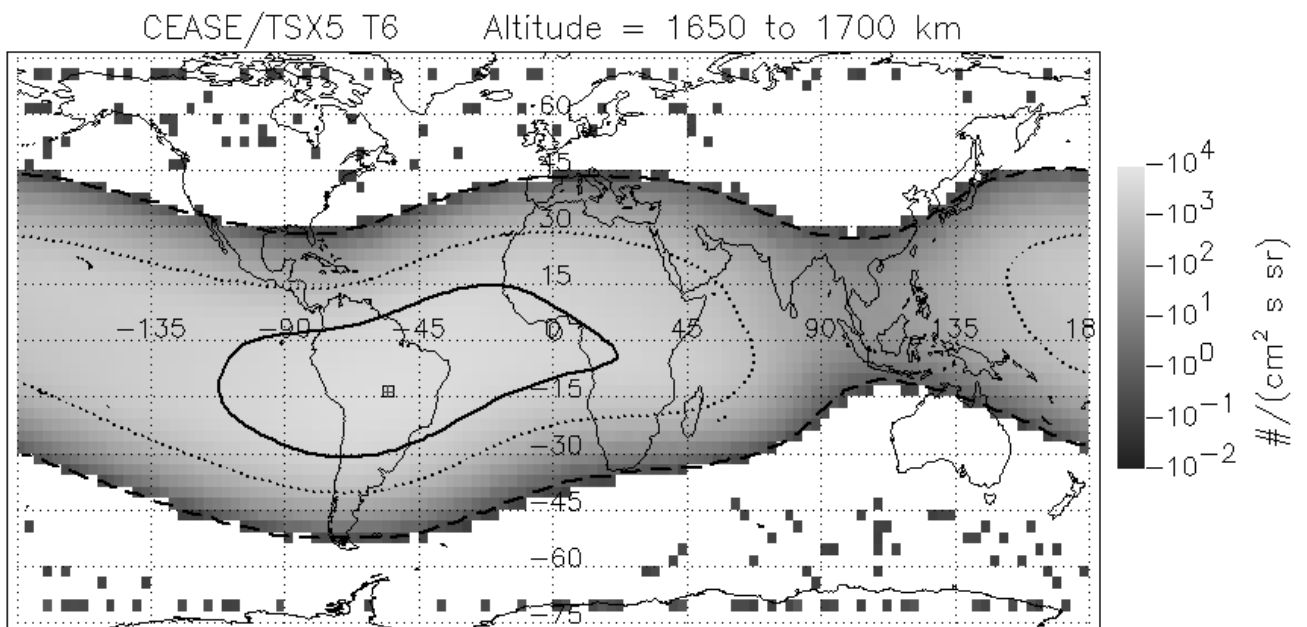


Fig. 1d. Flux intensity map for the > 38 MeV channel at 1650 km altitude.

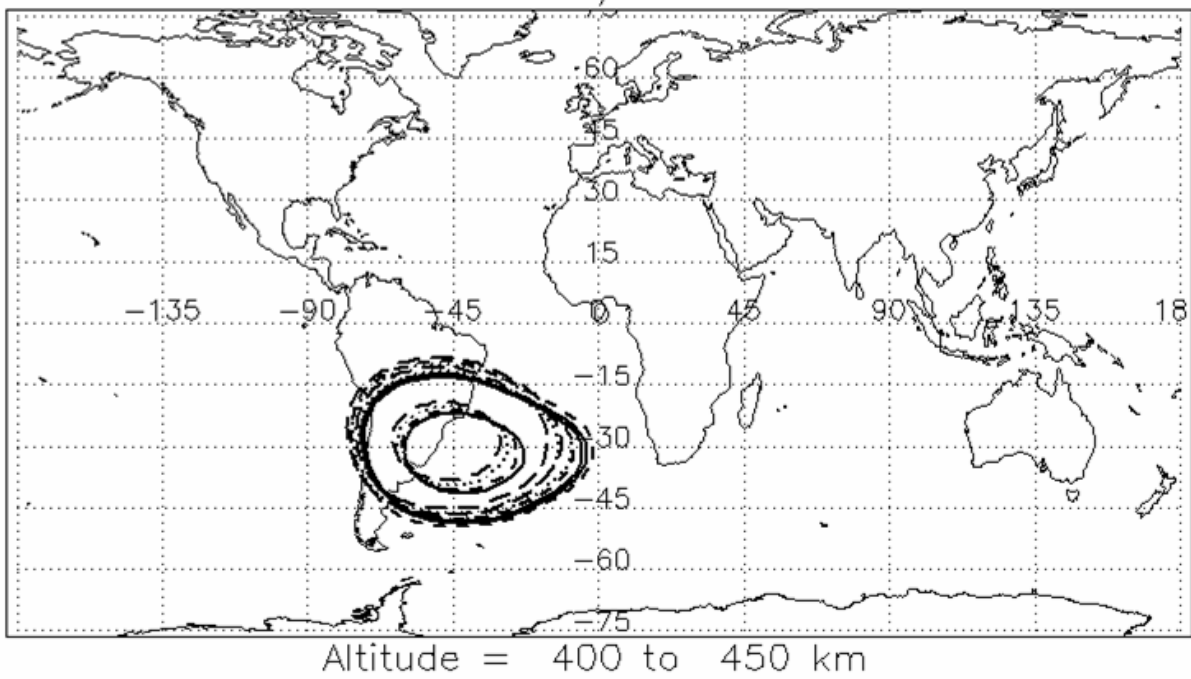


Fig. 2a. Boundary contours representing 1/2 maximum (inner most), 1/10 maximum (middle) and the  $3\sigma$  above background level for the > 23 MeV (solid curve), > 38 MeV (short dash curve), > 66 MeV (dot curve) and > 94 MeV (long dash curve) channels at 400 km.

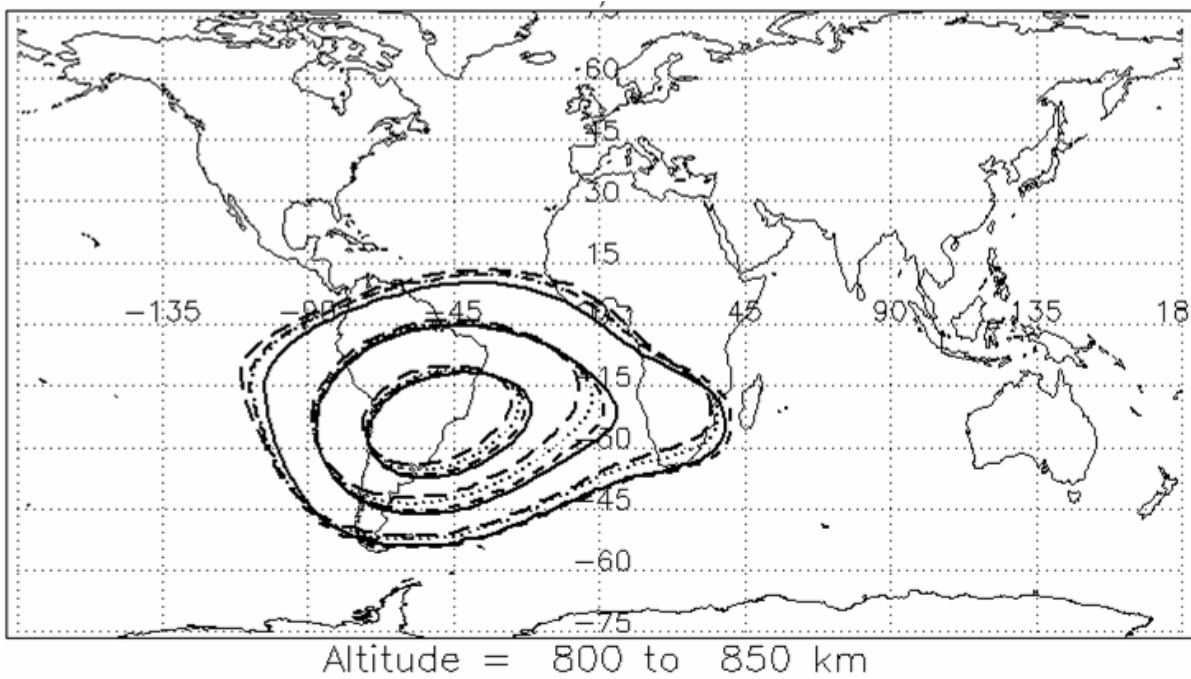


Fig. 2b. Boundary contours representing 1/2 maximum (inner most), 1/10 maximum (middle) and the  $3\sigma$  above background level for the > 23 MeV (solid curve), > 38 MeV (short dash curve), > 66 MeV (dot curve) and > 94 MeV (long dash curve) channels at 800 km.

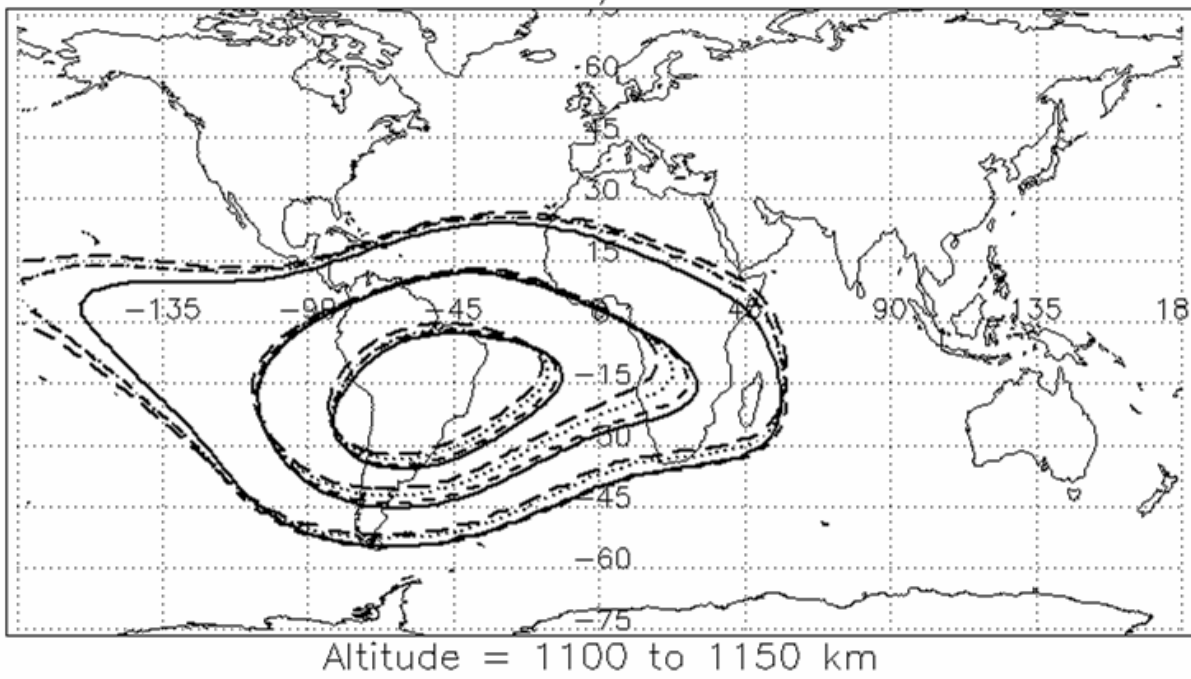


Fig. 2c. Boundary contours representing 1/2 maximum (inner most), 1/10 maximum (middle) and the  $3\sigma$  above background level for the  $> 23$  MeV (solid curve),  $> 38$  MeV (short dash curve),  $> 66$  MeV (dot curve) and  $> 94$  MeV (long dash curve) channels at 1100 km.

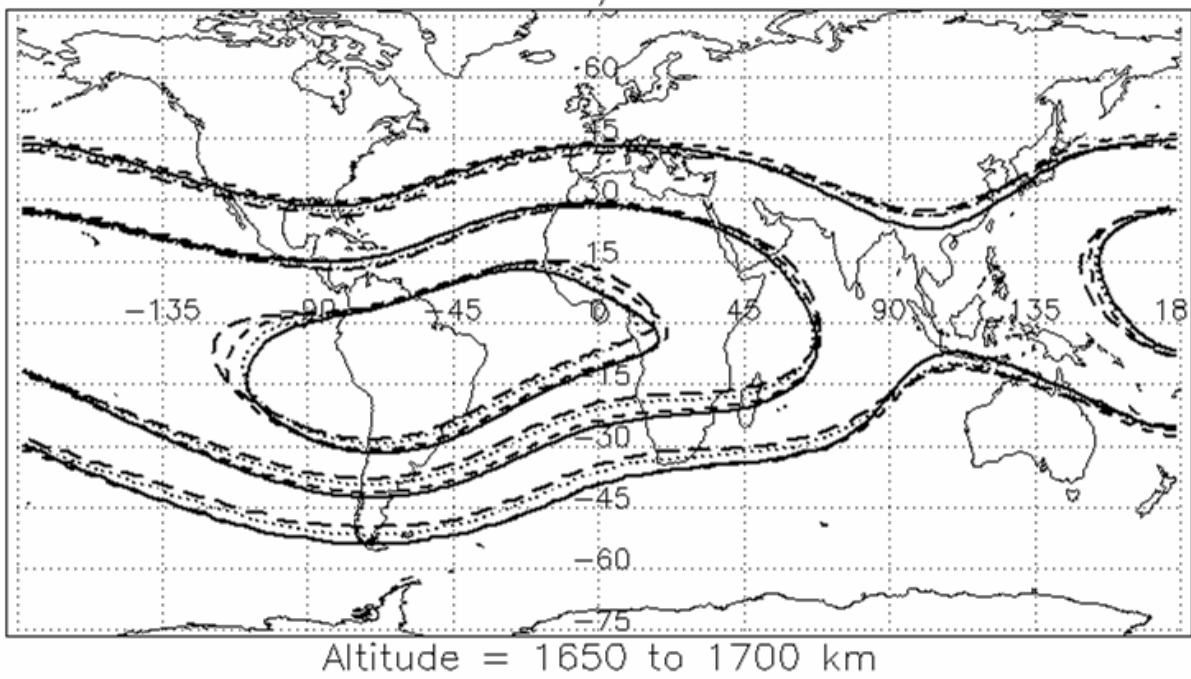


Fig. 2d. Boundary contours representing 1/2 maximum (inner most), 1/10 maximum (middle) and the  $3\sigma$  above background level for the  $> 23$  MeV (solid curve),  $> 38$  MeV (short dash curve),  $> 66$  MeV (dot curve) and  $> 94$  MeV (long dash curve) channels at 1650 km.

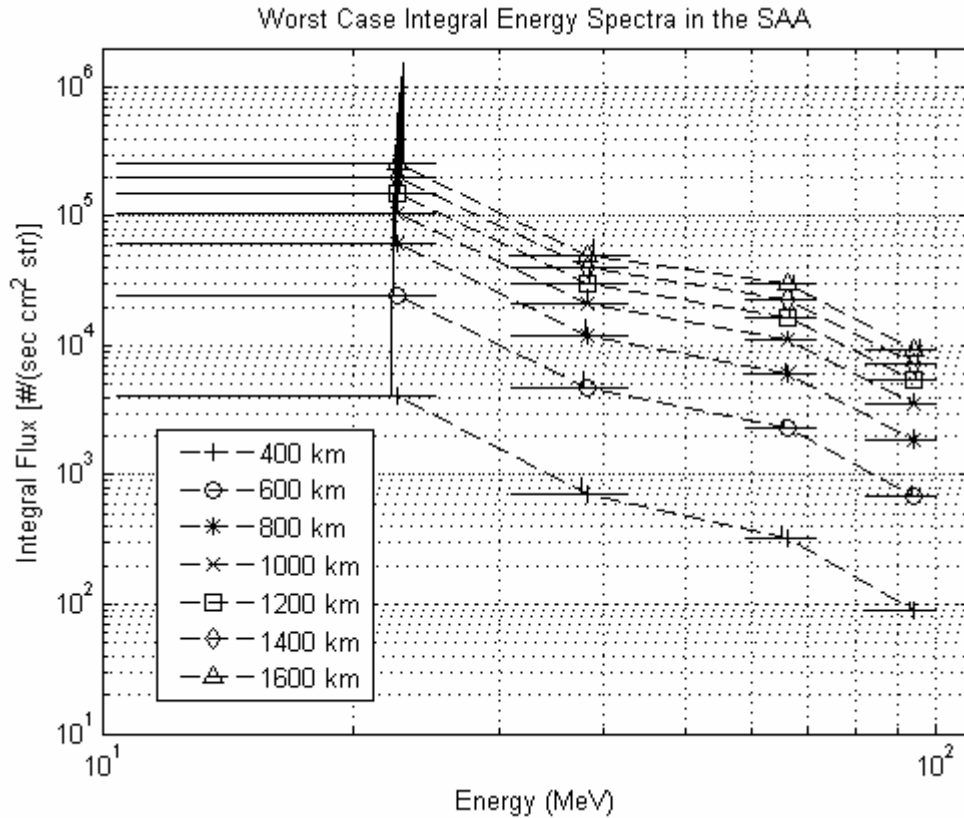


Fig. 3. Integral energy fluxes for the four channels at a sequence of altitudes between 400-1600 km. Vertical error bars have been offset slightly from the data points to aide in visualization.

### B. Integral Energy Spectra

From the maximum values of the integral fluxes recorded in each altitude range a worst case energy spectrum can be derived as function of altitude. Such spectra are shown in Fig. 3 for several altitudes between 400 to 1600 km. Error bars are indicative of the uncertainty resulting from the determination of threshold energies and geometric factors. There is a similarity in shape among spectra for all altitudes with a variation in intensity of a factor of approximately 25 from 400 to 1000 km but only 2.5 from 1000 to 1600 km. Below altitudes of  $\sim 1000$  to 1200 km effects of the atmospheric density become increasingly important as the density scale height approaches the order of the energetic proton cyclotron radius. Besides directional effects on the proton spectrum [8], the rapidly increasing magnitude of the atmospheric density (moving downwards) and consequent proton scattering cross-section reduces the overall proton intensity as evidenced in Fig. 3.

### C. Motion of the Anomaly

The relative motion of the SAA due to the variation of the Earth's internal field can be directly estimated by comparing data from the TSX-5/CEASE mission (8 June 2000 to 5 July 2006) to the data from the APEX/PASP mission (5 August 1994 to 13 May 1996), where the two missions have a  $\sim 8$

year center-to-center interval separation. Figure 4 shows a comparison of the 1/2 max (inner set) and 1/10 max (outer set) contours for the TSX-5  $> 38$  MeV (dot curve), TSX-5  $> 66$  MeV (dash curve), and APEX  $> 50$  MeV (solid curve) proton fluxes at 800 km altitude. It can be assumed that a  $> 50$  MeV contour in the TSX-5 epoch would lie between the  $> 38$  MeV and the  $> 66$  MeV contours shown.

The movement of the  $> 50$  MeV contour is apparent and the rate can be estimated by comparing the locations of the maximum fluxes. It is found to be between  $0.43 \pm 0.13$  deg/year (TSX-5  $> 38$  MeV maximum) and  $0.50 \pm 0.13$  deg year (TSX-5  $> 66$  MeV maximum) in a predominantly westward direction. Error bar estimates are based on the one degree bin size used to determine the maximum location. The observed rate is somewhat higher than previous estimates [2], [3] of  $\sim 0.3$  deg/yr though it is clear there is a noticeable dependence on energy and the characterization of the dosimeter channels used for this analysis, especially on APEX, is crude. The broad time window used for the TSX-5 average (6 years) also adds to the uncertainty.

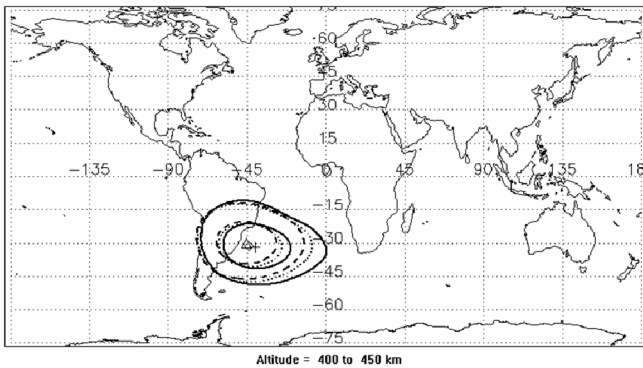


Fig. 4. Contours of the  $> 38$  MeV (dot curve) and  $> 66$  MeV (dash curve) integral flux from TSX-5 measured in the epoch 2000-2006 and the  $> 50$  MeV integral flux as measured in the epoch 1994-1996 by the APEX satellite (solid curve) at 400 km. The inner (outer) set marks the  $1/2$  ( $1/10$ ) maximum values which are located as indicated by the triangle ( $> 66$  MeV), circle ( $> 38$  MeV – almost underneath the triangle), and cross (APEX  $> 50$  MeV).

#### IV. SUMMARY

Proton flux intensity maps (Fig. 1) and boundary contours (Fig. 2) have been derived spanning the range of altitudes from 400 to 1650 km (in 50 km steps) and integral energies from  $> 23$  MeV to  $> 94$  MeV. Electronic versions of the full-color maps and contours can be obtained from the authors. An estimate of the worst-case integral spectra which can be experienced at a fixed altitude, i.e. the maximum flux point in each constant altitude map, has been derived (Fig. 3). It has been found that the location of the maximum region of the anomaly has moved westward consistent with the drift of the Earth's internal magnetic field.

One feature of energetic protons which has not been accounted for in constructing the maps is the anisotropic nature of the proton pitch-angle distribution. Given the finite field of view of CEASE there is the possibility that a proton distribution peaked sharply about the local mirror plane angle might not enter the detector at an angle to be efficiently detected. Examination of the TSX data indicates that this can occur below approximately  $-30$  degrees latitude. Initial analysis indicates the magnitude of this effect to be  $\sim 30$ - $50\%$  in the lower part of the anomaly. Work is currently underway to develop correction algorithms.

Though not perfect, it is hoped that the maps, boundaries and spectra provided in this report will aide in designing and operating spacecraft to better endure the hazards of the SAA.

#### V. REFERENCES

- [1] E. G. Stassinopoulos, "World Maps of Constant B, L, and Flux Contours", *NASA SP-3054*, Office of Technology Utilization, NASA, Washington, DC, 1970.
- [2] D. Heynderickx, "Comparison Between Methods to Compensate for the Secular Motion of the South Atlantic Anomaly", *Radiation Measurements*, vol. 26, pp. 369-373, 1996.
- [3] G. D. Badhwar, "Drift rate of the South Atlantic Anomaly", *J. Geophys. Res.*, vol. 102, pp. 2342-2349, 1997.
- [4] E. G. Mullen, G. P. Ginet, M. S. Gussenhoven and D. Madden, "SEE Relative Probability Maps for Space Operations", *IEEE Trans. on Nucl. Sci.*, vol. 45, pp. 2954-2963, 1998.
- [5] B. K. Dichter, J. O. McGarity, M. R. Oberhardt, V. T. Jordanov, D. J. Sperry, A. C. Huber, J. A. Pentazis, E. G. Mullen G. Ginet and M. S.

Gussenhoven, "Compact Environmental Anomaly Sensor (CEASE): a novel spacecraft instrument for in situ measurement of environmental conditions", *IEEE, Trans. on Nucl. Sci.*, vol. 45, pp. 2758, 1998.

- [6] D. Brautigam, et al., "Compact Environment Anomaly Sensor (CEASE): Response Functions", *Air Force Research Laboratory Technical Report AFRL-VS-HA-TR-2006-1030*, Hanscom AFB, MA, 2006.
- [7] D. Brautigam, "Compact Environment Anomaly Sensor (CEASE): Geometric Factors", in preparation.
- [8] G. P. Ginet, B. K. Dichter, D. H. Brautigam and D. Madden, "Proton Flux Anisotropy in Low-Earth Orbit", submitted for publication in *IEEE Trans. on Nucl. Sci.*, Jul 2007.
- [9] M. S. Gussenhoven, E. G. Mullen, M. D. Violet, C. Hein, J. Bass and D. Madden, "CRRES High Energy Proton Flux Maps", *IEEE Trans. on Nucl. Sci.*, vol. 40, pp. 1450-1457, 1993.